

文章编号: 0258-1825(2014)02-0258-06

Numerical simulation of parachute opening process in finite mass situation

CHENG Han¹, YU Li¹, YANG Xuesong², WANG Lu²

(1. College of Aerospace Engineering, Nanjing University of Aeronautics and Astronautics, Nanjing 210016, China;

2. Aviation key laboratory of science and technology on aeronautical life-support, AVIC Aerospace Life-support Industries LTD, Xiangyang 441000, China)

Abstract: In order to simulate the three-dimensional dynamic opening process of parachute system in a finite mass situation, a common flat circular parachute, the C9 parachute, is studied in this work. The working process (from inflating to dropping) of the C9 parachute is studied by using LS-DYNA based on the finite element theory. The calculation results are also verified by dropping test. The structure change and flow field change are obtained. Especially, the velocity and the acceleration of payload, which can reflect the deceleration characteristics of a parachute system, are also obtained by calculation in this work. Then the interrelation between dangerous section, overload and canopy shape is analyzed. The results show that the ALE method, a fluid-structure interaction method, can predict the deceleration characteristics and dangerous section during parachute opening. The results can reflect the general working laws of parachute in practice, and the method in this work can help determine the design or optimization of aerodynamic deceleration systems.

Key words: ADS; opening process; inflatable fabric; finite mass; parachute

中图分类号: V211.3

文献标识码: A

doi: 10.7638/kqdlxxb-2012.0101

0 Introduction

The inflatable fabric is widely used in aeronautics and astronautics with virtues of light weight and easy to fold. Especially, the parachute, a typical representative of inflatable fabric, occupies an irreplaceable position in aerodynamic deceleration field^[1-2]. The working principle is not complicated, but the inflation is a typical interaction of structure and fluid, which is a complex transient and nonlinear process. At present, the parachute design is mainly based on experience estimation, and verified by a large number of tests. The test is the ultimate examination, but it has high cost, high risk and long cycle. Moreover the test is difficult for data collection, especially difficult to get the dynamic change of fabric stress.

However, the numerical simulation is becoming an important research means due to its advantages of economy, flexibility and repeatability. From the 1980's, the researchers began to use the Fluid Structure Interaction (FSI) method to study the inflation process. The representative studies are as following. Purvis^[3] achieved the two-dimensional coupling calculation by simplified the canopy structure and fluid field model. Stein, Benney and Steeves^[4] proposed the CFD/MSD coupling model, which ignored the impact of fabric characteristics. Kim and Peskin^[5] used Immersed Boundary (IB) method to simulate the three-dimensional parachute in finite mass situation, but there are no results such as overload, structure stress. Ben and Roland^[6] explored the Arbitrary Lagrange Euler (ALE) method to simulate the complete working process. Kenji^[7] used Stabilized Space-

* 收稿日期: 2012-06-14; 修订日期: 2012-11-14

基金项目: 国家自然科学基金(11172137)资助项目, 航空科学基金(20122910001)

作者简介: 程涵(1984-), 男, 博士研究生, 主要研究方向: 柔性织物流固耦合. E-mail: chenghanstorm@sina.com

通讯作者: 余莉, 女, 博士, 教授, 博士生导师. E-mail: yuli_happy@163.com

引用格式: 程涵, 余莉, 杨雪松, 等. 有限质量情况下降落伞开伞过程数值仿真研究(英文)[J]. 空气动力学学报, 2014, 32(2): 258-263. doi: 10.7638/kqdlxxb-2012.0101. CHENG H, YU L, YANG X S, et al. Numerical simulation of parachute opening process in finite mass situation[J]. ACTA Aerodynamica Sinica, 2014, 32(2): 258-263.

Time FSI (SSTFSI) method to obtain the structure and fluid results of a parachute in a steady-state. Most previous studies are emphasized on flow field calculation in infinite mass situation (the situation in which deceleration effect can be negligible is called as infinite mass situation, otherwise, is called as finite mass situation; the latter not only to consider the effect of flow field and structure but also consider the flight characteristics of parachute; the latter need wider computational domain and be more sensitive to the coupling coefficient than the former). There are fewer studies on the fabric structural mechanics analysis; the studies on structural analysis of entire working process (from inflating process to dropping process) are even fewer. The articles about the relationship between deceleration characteristics and fabric mechanical mechanism are not yet open.

The finite element method takes the dominant position in CSD, and also can be used in CFD. The finite difference method or finite volume method is mainly used in CFD that is why the most previous studies are emphasized on flow field analysis, and those studies are helpless for fabric analysis. The main purpose of this work is analyzing the fabric and flow field dynamic change in a finite mass situation and providing reference for Aerodynamic Deceleration System (ADS) design or optimization. Therefore the entire working process of parachute is simulated by using LS-DYNA based on finite element method.

1 Model development

1.1 Governing equations

1.1.1 The governing equations and boundary conditions of flow field

The governing equations of mass, momentum and energy based on ALE description^[8-9] are as flows:

$$\frac{\partial \rho}{\partial t} = -\rho \frac{\partial v_i}{\partial x_i} - w_i \frac{\partial \rho}{\partial x_i} \quad (1)$$

$$\rho \frac{\partial v_i}{\partial t} = \sigma_{ij,j} + \rho b_i - \rho w_j \frac{\partial v_i}{\partial x_j} \quad (2)$$

$$\rho \frac{\partial E}{\partial t} = \sigma_{ij} v_{i,j} + \rho b_i v_i - \rho w_j \frac{\partial E}{\partial x_j} \quad (3)$$

Where v_i and w_i are the material and reference velocities, respectively, and $w_i = v_i - \hat{v}_i$, \hat{v}_i is mesh velocity. The stress tensor σ_{ij} is described as $\sigma_{ij} = -p\delta_{ij} + \mu(v_{i,j} + v_{j,i})$, and δ_{ij} is Kronecker's delta function. b_i denotes

body force.

The relationship of Lagrangian, Eulerian, and referential coordinate is as follows:

$$\frac{\partial f(X_i, t)}{\partial t} = \frac{\partial f(x_i, t)}{\partial t} + w_i \frac{\partial f(x_i, t)}{\partial t} \quad (4)$$

Where X_i is the Lagrangian coordinate, and x_i is the Eulerian coordinate.

The boundary conditions are:

$$v_i = \bar{v}_i, \quad \text{on } \Gamma_D$$

$$\sigma_{ij} n_j = 0, \quad \text{on } \Gamma_N$$

Where, Γ_D and Γ_N are Dirichlet and Neumann boundary conditions, respectively.

1.1.2 The governing equations and boundary conditions of structure

$$\rho^s \frac{d^2 u_i}{dt^2} = \sigma_{ij,j} + \rho^s b_i \quad (5)$$

Where u_i denotes displacement, and ρ^s the density of structure. Here the body force b_i only at z component contains the gravity acceleration g .

The boundary conditions are:

$$u_i = \bar{u}_i, \quad \text{on } \Gamma_U$$

$$\sigma_{ij} n_j = \bar{F}_i, \quad \text{on } \Gamma_F$$

1.1.3 The dynamics equation of recycled goods

For calculating conveniently, the deceleration characteristic of recycled goods is ignored. The dynamics equation is:

$$m \cdot \frac{d\mathbf{u}}{dt} = \mathbf{G}_w + \mathbf{F}_{\text{dynamic}} \quad (6)$$

Where \mathbf{G}_w is a constant vector, and denotes the gravity of recycled goods; $\mathbf{F}_{\text{dynamic}}$ denotes parachute dynamic load^[10-11].

1.2 Coupling method

The governing equations above are solved using time explicit method based on central difference, which can provide second-order time accuracy. The velocity and displacement of structure and flow field of coupling domain are updated with following equations:

$$\mathbf{u}^{n+1/2} = \mathbf{u}^{n-1/2} + \Delta t \cdot \mathbf{M}^{-1} \cdot (\mathbf{F}_{\text{ext}} + \mathbf{F}_{\text{int}}) \quad (7)$$

$$\mathbf{x}^{n+1} = \mathbf{x}^n + \Delta t \mathbf{u}^{n+1/2} \quad (8)$$

Where, \mathbf{F}_{int} and \mathbf{F}_{ext} are internal and external force vector, and \mathbf{M} is the mass matrix.

The structure and flow field are coupled by penalty function. \mathbf{F}_c , the interface force is calculated based on $\mathbf{F}_c = k \cdot \mathbf{d}$ (here, \mathbf{d} denotes distance of coupling point, and k denotes the stiffness coefficient). In order to achieve

coupling, the speed and displacement of coupling domain are adjusted based on F_c , which is a part of F_{ext} .

2 Simulation model

This C9 parachute model was established in full scale. The main parameters of C9 parachute are shown in Table 1. The kinds of fabric material can be see in the reference[10].

Table 1 Parameters of model

表 1 模型参数

Number of canopy gores	28
Diameter of vent (m)	0.853
Nominal area (m ²)	57.2
Density of canopy (kg/m ³)	533
Elastic modulus of canopy (Pa)	4.3e8
Thickness of canopy (m)	1e-4
Density of line (kg/m ³)	462
Elastic modulus of line (Pa)	9.7e10
Length of line (m)	7

The fabric permeability was considered by using anisotropic Ergun porous flow model, the porous coupling forces were derived from the integration of the Ergun Equation on the shell volume^[12]:

$$\Delta P = (av' + bv'^2) \cdot e \quad (9)$$

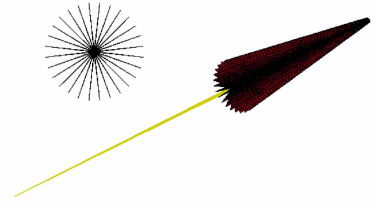
Where a and b denote viscosity coefficient and inertia coefficient of fabric, they are 1.599×10^6 kg/m³ and 4.805×10^5 kg/m⁴ in this work. e is the fabric thickness, v' denotes average flow velocity through fabric.

The canopy and lines were meshed by 20,000 sell elements and 2,300 rope elements respectively, and 600,000 hexahedral elements were used to mesh the flow field. The structural elements inserted in the flow field elements which were set as non-reflecting boundary. The gravity of recycled goods loaded on the focal point of all lines. The finite element model is shown in figure 1. The entire calculation consumes 400 hours by using a workstation (the DAWNING I650r-F).

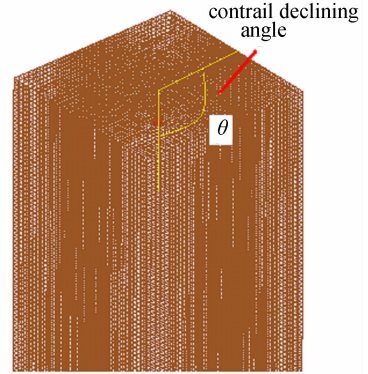
In order to compare the simulation results with the test^[11], the calculation condition is shown in Table 2. The weight of recycled goods was derived by $W_T/S_0 = 17.7N/m^2$ (the data of this reference are statistical results based on a large number of tests, which are representative and authoritative in ADS field).

3 Test verification

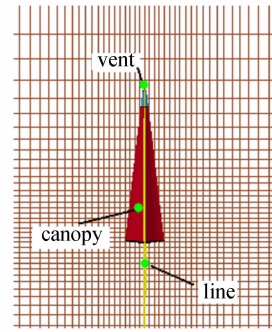
The reference [11] provided the canopy shape change and dimensionless load. The figure 2 is the comparison of calculation and test. The t_f was 1.4s in calcu-



(a) Canopy and lines



(b) Parachute and flow field



(c) Partial enlarged view of mesh

Fig. 1 Finite element model of parachute

图 1 降落伞有限元模型

Table 2 Working conditions of calculation

表 2 计算工况

Opening altitude(m)	1830
Atmospheric pressure(Pa)	8.12e4
Atmospheric density(kg/m ³)	1.023
Payload(N)	980
Snatch velocity(m/s)	20
Contrail declining angle(°)	90

lation results. When the canopy was inflated, the average projected area was 25.2 m². At 1.4s, this value was reached first time, therefore the moment ($t = 1.4s$) was defined as t_f according to the definition in the reference^[11]. The F shown in ordinate title is the component force of the resultant ($G_w + F_{dynamic}$) on Z direction.

It can be found that the calculation results were consistent with the dropping test. The first peak (FP) appeared after the canopy top had been completely expanded (P2), and the second peak (SP) appeared

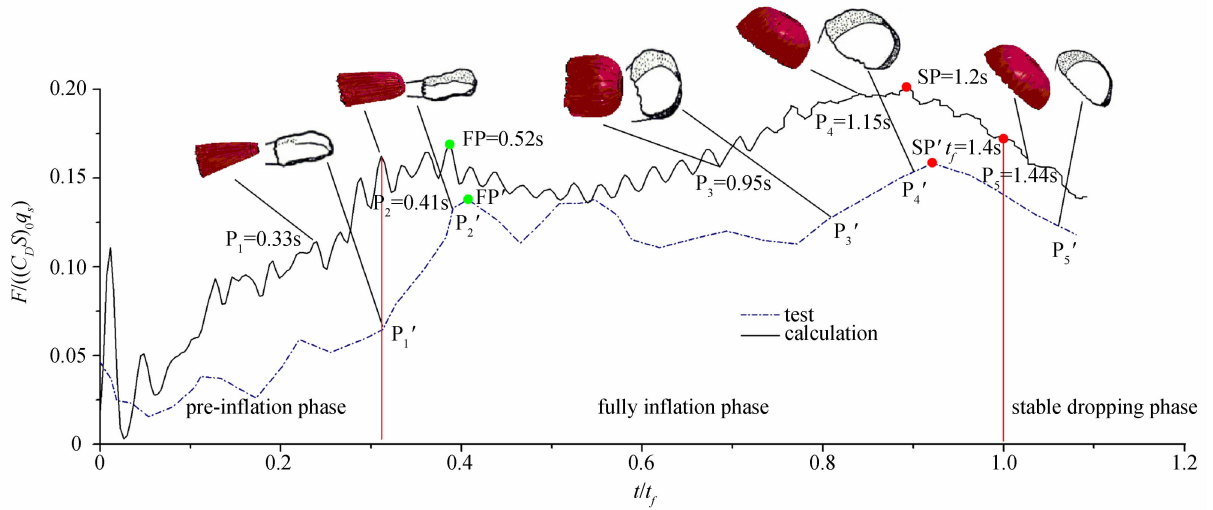


Fig. 2 Results comparison of calculation and dropping test

图 2 计算和空投试验结果对比

soon after the canopy was inflated the first time (P4). Then the canopy load continued to decline, the canopy would be over inflated and appeared a biggest projected area at a given moment.

We also found that the dimensionless load curve of calculation was slightly higher than the test curve, because the contrail declining angle in this work was 90° while the test angle was less than 90°. It is proved that the dynamic load of 90° is greater than other angles based on a large number of tests.

4 Analysis of calculation results

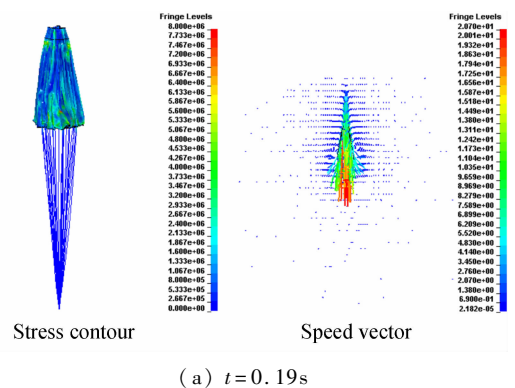
4.1 Structure and flow field change

Figure 3 shows the equivalent stress, flow velocity. Figure 4 shows the velocity and acceleration of recycled goods.

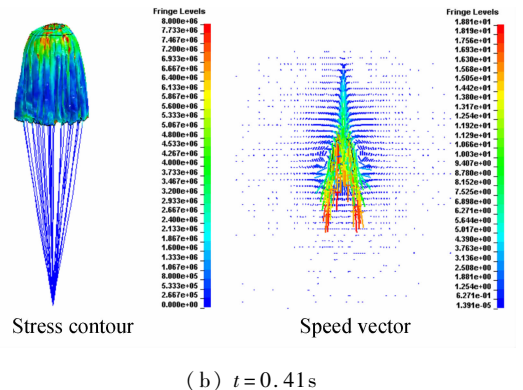
According to the change of parachute shape, the entire working process can be divided into three phases: pre-inflation phase (0 ~ 0.41s), fully inflation phase (0.41 ~ 1.4s), stable dropping phase (after 1.4s).

The pre-inflation phase (0 ~ 0.41s): The canopy bottom was opened firstly, and airflow into the canopy easily. The canopy inflated uniformly (Fig. 3a). At 0.41s, most of canopy was in folded state, while the canopy top completely opened, which denoted the end of the pre-inflation phase. But the first peak of acceleration appeared at 0.52s, which was consistent with the description in reference[11].

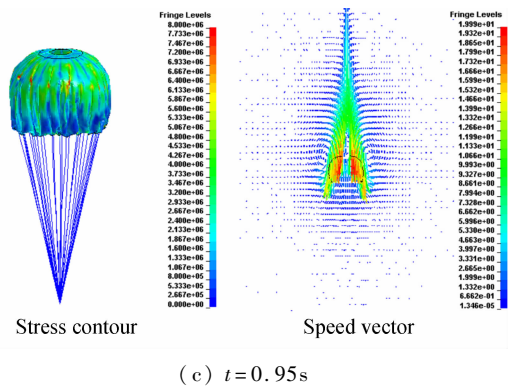
The fully inflation phase (0.41 ~ 1.4s): After the



(a) $t = 0.19s$



(b) $t = 0.41s$



(c) $t = 0.95s$

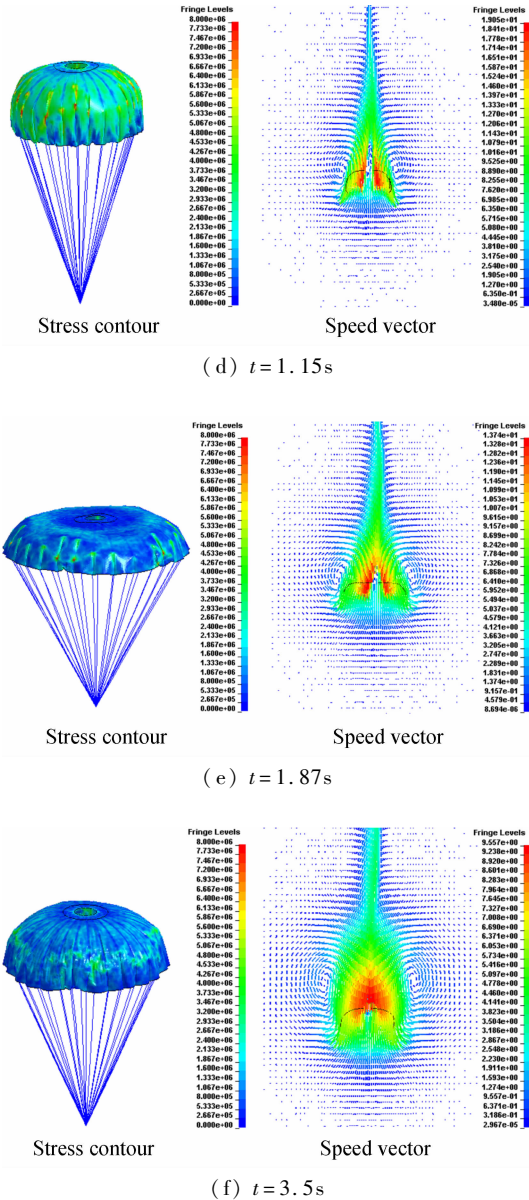


Fig. 3 Results of structure and flow field

图3 结构和流场结果

first phase, the canopy appeared “squid” shape. The canopy expanded from top to bottom gradually.

At 1.2s, the recycled goods bore the maximum overload (Fig. 4). Until 1.4s, the canopy achieved the fully inflated shape first time, which was same with the conclusion in reference[13].

The stable dropping phase (after 1.4s): The canopy appeared top collapse due to the fabric elastic deformation (Fig. 3e). Then the top collapse was recovered and appeared the slightly “breathing” phenomenon. The acceleration of the recycled goods tended to 0m/s^2 , and the velocity maintained at 6.2m/s gradually. The dropping velocity was consistent to the actual stable dropping velocity about $6 \sim 7\text{m/s}$.

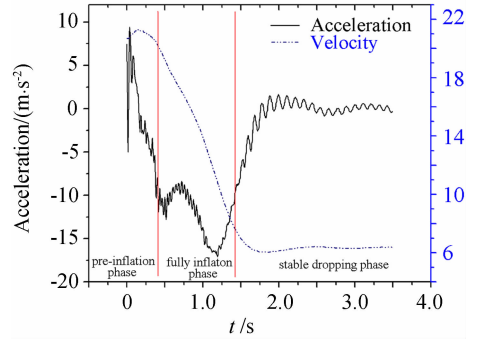


Fig. 4 Acceleration and velocity of payload

图4 载荷加速度和速度

4.2 Stress change on parachute meridian

In order to more effectively analyze the fabric structural change, the stress change on parachute meridian was studied (the five elements shown in Figure 5 were located at five different parts: the canopy top, the upper middle part, the middle part, the lower middle part and the bottom part).

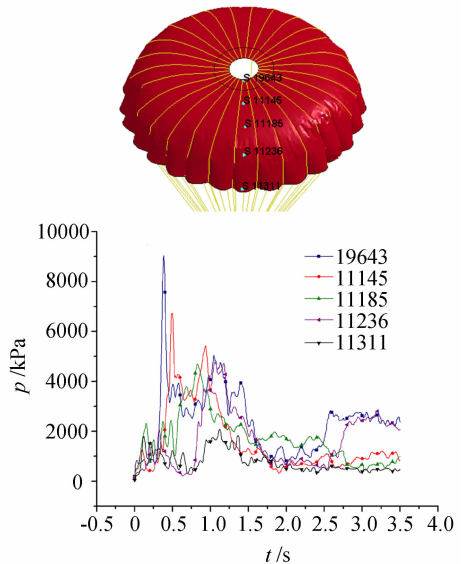


Fig. 5 The positions and equivalent stress of five elements on parachute meridian

图5 伞衣子午线上五个单元位置及等效应力

(1) In pre-inflation phase ($0 \sim 0.41\text{s}$), the maximum stress would appear at the end of the pre-inflation. The stress concentrated on the top part, which may be the weakest part during the whole process, especially at the area where the folds began to expand (Fig. 3b).

(2) In fully inflation phase ($0.41\text{s} \sim 1.4\text{s}$), with the canopy fully inflated from top to bottom, the stress peak appeared on the upper middle part, middle part, and lower middle part successively. The top part and the upper middle part even appeared the second peak which is lower than the first peak. After these canopy parts ap-

peared the stress peak in turn, the recycled goods appeared the second acceleration peak at 1.2s, this lag phenomenon is caused by fabric elasticity.

(3) In stable dropping phase (after 1.4s), the canopy appeared top collapse and the canopy stress began to shrink, and the stress mainly concentrated on the middle part. After the top collapse recovered (after 2.5s), the aerodynamic drag was mainly produced by canopy top. The lower and middle surface kept bending stably and the stress of which was recovered.

5 Conclusions

In this paper, the entire working process of C9 parachute was simulated by using LS-DYNA based on finite element method, and the calculation results are verified by test. The conclusions are as following:

(1) There were two peaks on the curve of dynamic load or acceleration. The first peak appears after the canopy was opened, and the second peak appears before the canopy was fully inflated. But the peak value was affected greatly by the initial canopy shape and outside conditions.

(2) Both of the two peaks would cause the fabric stress increasing. The dangerous moment of the canopy appears at the end of the pre-inflation rather than at the maximum overload moment and the dangerous section is the canopy top. The result can be guidance for the fabric selection or ADS optimization.

(3) There are many other factors affecting the canopy stress such as wind direction, fully folded and so on. Moreover the fabric material model is simple in this work. On the other hand, how to select fabric material

or optimize ADS according to the simulation results need to a further study. These issues remain to be studied in future.

References:

- [1] YU L, MING X. Study on transient aerodynamic characteristics of parachute opening process[J]. *ACTA Mechanica Sinica*, 2007, 23(6): 627-633.
- [2] YU L, SHI X L, MING X. Numerical simulation of parachute during opening process[J]. *ACTA Aeronautica et Astronautica Sinica*, 2007, 28(1): 52-57.
- [3] PURVIS J W. Theoretical analysis of parachute inflation including fluid kinetics[R]. AIAA 81-1925, 1981.
- [4] STEIN K R, BENNEY R J, STEEVES E C. A computational model that couples aerodynamic structural dynamic behavior of parachutes during the opening process[R]. NASA ADA 264115, 1993.
- [5] KIM Y S, PESKIN C S. 3-D parachute simulation by the immersed boundary method[J]. *Computers and Fluids*, 2009, 38: 1080-1090.
- [6] BEN T, ROLAND S. Finite mass simulation techniques in LS-DYNA[R]. AIAA 2011-2592, 2011.
- [7] KENJI T. Fluid structure interaction modeling of spacecraft parachutes for simulation-based design[J]. *Journal of Applied Mechanics*, 2012, 79: 1-9.
- [8] SOULI M, OUAHSINE A, LEWIN L. ALE formulation for fluid-structure interaction problems[J]. *Computer Methods in Applied Mechanics and Engineering*, 2000, 190: 659-675.
- [9] CASADEI F, HALLEUX J P, SALA A, et al. Transient fluid-structure interaction algorithms for large industrial applications[J]. *Computer Methods in Applied Mechanics and Engineering*, 2001, 190: 3081-3110.
- [10] CALVIN K L. Experimental investigation of full-scale and model parachute opening[R]. AIAA 1984-0820, 1984.
- [11] EWING E G, KNACKE T W, BIXBY H W. Recovery systems design guide[M]. Beijing: Aviation Industry Press, 1988.
- [12] AQUELET N, WANG J, TUTT B A, et al. Euler-lagrange coupling with deformable porous shells[C]. ASME Pressure Vessels and Piping Division Conference. Vancouver BC Canada, 2006.
- [13] RONG W, CHEN X, CHEN G L. The study of the parachute opening load in low atmospheric density[J]. *Spacecraft Recovery and Remote Sensing*, 2006, 27(4): 7-11.

有限质量情况下降落伞开伞过程数值仿真研究

程 涵¹, 余 莉¹, 杨雪松², 王 璐²

(1. 南京航空航天大学 航空宇航学院, 南京 210016;

2. 航宇救生装备有限公司 航空防护救生航空科技重点实验室, 襄阳 441000)

摘 要:为了模拟降落伞减速系统在有限质量情况下的三维动态开伞过程,以典型平面圆形伞 C9 伞为例,采用 LS-DYNA 基于有限元理论的 ALE 流固耦合方法对其充气至稳降过程进行研究,并用空投试验验证计算结果。计算获得了结构、流场动态变化,还获得了反映减速特性的载荷速度、加速度变化情况,分析了降落伞工作过程中危险截面、过载及外形之间的对应关系。研究结果表明:ALE 法能够预测伞衣展开过程中减速特性以及危险截面,数值结果反映了实际工作过程的一般规律。

关键词:气动减速系统;开伞过程;充气织物;有限质量;降落伞